



A New Wavelet Packet Based Method for Adaptive Single Pole Auto-Reclosing

Navid Ghaffarzadeh

Sadegh Jamali

Electrical Engineering Department
Iran University of Science and Technology
Tehran

Keywords : Adaptive auto-reclosure, Permanent fault, Secondary arc,
Transient fault, Transmission line, Wavelet packet transform

Abstract :

A novel and simple approach for adaptive single pole auto-reclosing is proposed in this paper. The algorithm consists of capturing the faulted phase voltage using 20kHz sampling rate, decomposing it by db8 wavelet packet to attain the coefficients of nodes 257, 259 to 262 and defining an Index, which is obtained from the sum of the coefficients energy of nodes 257, 259 to 262. Finally, by evaluating the value of the Index, the transient, permanent faults and the secondary arc extinction instant can be identified. The significant advantage of the proposed algorithm is that it does not need variant threshold level and therefore its performance is independent of fault location, line parameters and the system operating conditions. Moreover, it can be used in the transmission lines with reactor compensation. The proposed method has been successfully tested under a variety of fault conditions on a 500KV overhead line using PSCAD/EMTDC

software. The test results validate the algorithm ability in distinguishing between transient and permanent faults and determining the instant of secondary arc extinction.

I. INTRODUCTION

The most common faults on overhead lines are transient, with more than 90% of these are single phase to earth faults. For such faults, single pole auto-reclosing (SPAR) provides a means of improving transient stability and reliability. Furthermore, half the pre-fault power can be transferred in the remaining healthy phases [1-2].

The classical automatic reclosing techniques employs a prescribed reclosure time, that is, the breaker is re-closed after a fixed period following a tripping operation. However employing a fixed prescribed dead time can pose problems. In the case of an arcing fault, for example, a fault restrike due

to insufficient time for the fault path to fully de-ionise can threaten system stability and reliability. On the other hand, unsuccessful reclosing during a permanent fault may aggravate the potential damage to the system and equipment [3]. For some extra-high-voltage lines, especially near generating plants, the classical automatic reclosing of breakers cannot be used and therefore adaptive reclosing schemes have been introduced over the past decades [4]. Such schemes prevent unsuccessful reclosing on permanent faults, and during transient (arcing) faults reclosing is done only after full extinction of the secondary arc and complete de-ionisation of the arc path.

Many methods have been proposed for SPAR. In [5] the value of voltage induced from healthy phases to the faulted one is used. In [2] the root mean square (RMS) value of faulted phase is calculated over a period and when the difference between present RMS and the previous one at each time step attains a value above a certain threshold level, a reclosing command signal is generated. Reference [3] uses the current of one of the two healthy phases and compares its power of high frequency components with a threshold level.

In [6] a criterion of a dual-window transient energy ratio based on mode current is presented. In this paper, it is shown that the energy ratio approaches unity during steady-state operation whilst it increases greatly during the fault conditions, existences of primary and secondary arcs and arc extinguishing. Furthermore, the same authors in [7] propose a criterion called a dual-window transient energy ratio based on the faulted phase voltage.

References [8-10] present different adaptive autoreclosure approaches based on artificial neural network (ANN). In [8] by use of Fourier Transform various components of the faulted phase voltage is extracted and applied to an ANN, which is trained by more than 25000 permanent and transient single phase to earth faults.

In [9] the Short Time Fourier Transform (STFT) is employed to extract proper feature vectors, which are the energy of voltage waveform in five frequency bands and are applied in training the ANN. The network has five inputs, one hidden layer and an output layer with one node. Hybrid schemes using neural networks and wavelet transform are suggested in [10]. In this paper, the wavelet transform is used to extract feature vectors and the vectors are used as input of ANN to identify the transient, permanent faults and the secondary arc extinction instant. Authors of [11] use Fuzzy Logic concept to distinguish permanent faults from the transient.

In [12] the total harmonic distortion (THD) value of the faulted phase voltage is used to determine an appropriate time for reclosing. The fundamental component of the zero sequence power at both ends of a line is used in [13] to detect the extinction time of the secondary arc. Authors of [14] present a new method for SPAR based on the zero sequence voltage.

This paper introduces a new algorithm for adaptive single-pole auto-reclosing based on wavelet packet transform (WPT). In the algorithm, the faulted phase voltage is captured with a sampling rate of 20kHz. Then the db8 wavelet packet is used to decompose the signal to level 8 and to define an Index, which is obtained from the sum of the coefficients energy of nodes 257, 259 to 262. Finally, by evaluating the value of the Index, the transient, permanent faults and the secondary arc extinction instant can be identified. The proposed algorithm does not require an artificial intelligence tool like ANN nor does it need variant threshold level, so its results are independent of the system and fault conditions. The algorithm can also be used in transmission systems with reactor compensation.

The rest of this paper is organized as follows. In section II wavelet packet transform is introduced, Section III presents the simulated system parameters. In Section

IV arcing fault modeling is briefly introduced. Section V indicates the proposed algorithm and demonstrates how the proposed Index is calculated. Simulation results and conclusion are presented in Section VI and VII, respectively.

II. WAVELET PACKET TRANSFORM

The wavelet Packet Transform (WPT) is a generalized version of the discrete wavelet transform in a way that each level of resolution (also known as octave) j consists of 2^j boxes, generated by a tree of low pass and high pass filtering operations. Therefore, the frequency bandwidth of a box decreases with growing octave number. In other words, with increasing octave number, the frequency resolution becomes higher while the time resolution is reduced. Starting with the signal $f[n]$ with length N , the first level decomposition will produce $d^1[n]$ and $a^1[n]$ as any other wavelet transform. The second level decomposition will produce four sub-bands due to the decomposition of both $d^1[n]$ and $a^1[n]$ using the same set of filters used in the first level decomposition. These four sub-bands are $aa^2[n/2]$, $ad^2[n/2]$, $da^2[n/2]$, and $dd^2[n/2]$ [15], [16], [17]. Thus the ordinary wavelet decomposition is a sub-tree of the wavelet packet decomposition tree. The main advantages of the WPT over other types of wavelet transforms are accurate and detailed representations of the decomposed signals. Also, wavelet packet basis functions are localized in time offering better signal approximation and decomposition. These basis functions are generated from one base function (the mother wavelet $\psi(t)$ or the scaling function $\varphi(t)$ if exists) at scale, oscillation and location given as [15], [16].

$$w_{s,c,b}(n) = 2^{j/2} W_C(2^{-j}(n-b)) \quad (1)$$

where $W_C(n)$ is the wavelet transform coefficient matrix.

In wavelet packet analysis, a signal $f[n]$ is represented as a sum of orthogonal wavelet packet basis functions $w_{s,c,b}(n)$ at different scales, oscillations and locations given as [15], [16].

$$f[n] = \sum_S \sum_C \sum_b w_{s,c,b}[n] W_C[n] \quad (2)$$

The WPT has many applications including pattern recognitions, image processing, denoising, data compression and others [17], [19]. The WPT has a decomposition tree shown in Fig. 1 that employs the DWT as part of its decomposition process [19].

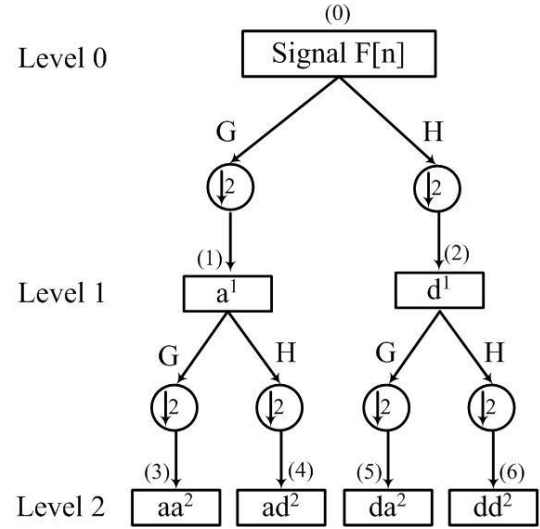


Fig. 1 WPT Decomposition of the signal $f[n]$.

The vectors G and H stand for the low pass and high pass filters, respectively determined by the mother wavelet. The coefficients of G and H are not independent from each other, rather they are related through the following relation [15],[17],[20].

$$h_k = (-1)^k g_{L-k}; \quad k = 0,1,2,\dots,L-1 \quad (3)$$

Any filter bank that satisfies the relation in Eq. 1 is known as a quadrature mirror filter (QMF) bank [15], [17], [20], [21].

The first level two sub-bands can be expressed as [17], [18].

$$a^1[n] = \sum_{k=0}^{N-1} g(k) f(n-k) \quad (4)$$

$$d^1[n] = \sum_{k=0}^{N-1} h(k) f(n-k) \quad (5)$$

The first level details d^1 represent high frequencies present in the analyzed signal $f[n]$. In general, the details represent high frequency components extracted from the analyzed signal at each level of resolution

[14], [18]. It should be noted that in wavelet packet analysis, a^1 and d^1 are called as nodes 1 and 2 respectively.

The second level four subbands can be expressed mathematically as.

$$aa^2[n] = \sum_{k=0}^{N/2-1} g(k)a^1(n-k) \quad (6)$$

$$ad^2[n] = \sum_{k=0}^{N/2-1} h(k)a^1(n-k) \quad (7)$$

$$da^2[n] = \sum_{k=0}^{N/2-1} g(k)d^1(n-k) \quad (8)$$

$$dd^2[n] = \sum_{k=0}^{N/2-1} h(k)d^1(n-k) \quad (9)$$

It is noteworthy that, aa^2 , ad^2 , da^2 and dd^2 are called as nodes 3, 4, 5 and 6 respectively.

This procedure is repeated until the signal is decomposed to a pre-defined certain level.

III. SIMULATED SYSTEM PARAMETERS

Fig. 2 shows the single line diagram of a 500kV transmission line. Power system frequency is 60Hz. The 260km transmission line is modeled using the Frequency Dependent (Phase) Model.

Fig. 3 depicts the line construction considered.

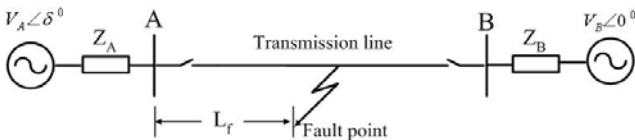


Fig. 2 Single line diagram of the simulated system.

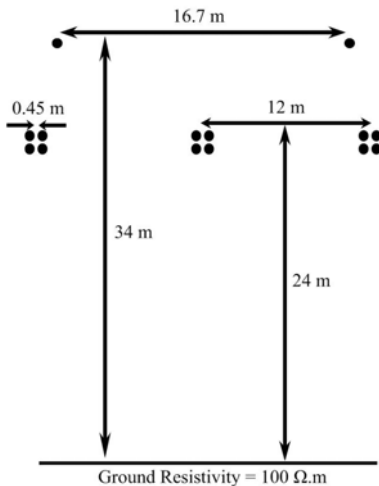


Fig. 3 Transmission-line conductors geometry.

Each source is modeled by simple lumped parameter networks based upon the symmetrical short-circuit level (SCL) and sequence impedance ratios Z_{S0} / Z_{S1} at power frequency. The value of SCL and Z_{S0} / Z_{S1} in the two buses is as follows:

$$SCL_A = 1500 \text{ MVA}, Z_{S0A} / Z_{S1A} = 1 \quad (10)$$

$$SCL_B = 5000 \text{ MVA}, Z_{S0B} / Z_{S1B} = 1 \quad (11)$$

IV. MODELING FOR ARCING FAULT

Several arcing fault models have been proposed in the literature. Modeling techniques for arc phenomena have improved by field experiments to simulate dynamic characteristics [22, 23].

In this paper, arcing faults have been modeled as presented in [23]. From a modeling point of view, arcing faults can be classified as high current primary arc during the fault and low current secondary arc after the faulted phase is isolated. The secondary arc is sustained by mutual coupling between the healthy and faulted phases [23].

A. Primary arc

It can be shown that the primary arc model is represented by a time dependent resistance as follows:

$$\frac{dg_p}{dt} = \frac{1}{T_p} (G_p - g_p) \quad (12)$$

where g_p is the time varying primary arc conductance, T_p is the time constant of the primary arc and G_p is the stationary primary arc conductance.

The stationary primary arc conductance can be defined as:

$$G_p = \frac{|i|}{V_p \ell_p} \quad (13)$$

where V_p is the constant voltage parameter per unit length of the primary arc, ℓ_p is the primary arc length and $|i|$ is absolute value of the primary arc current.

The time constant of the primary arc can be evaluated by

$$T_p = \frac{\alpha_p I_p}{I_p} \quad (14)$$

where the coefficient α_p is about 2.85×10^{-5} for the arc currents ranging from 1.4kA to 24kA [23].

B. Secondary arc

The secondary arc is a highly complex phenomenon, and is influenced by a number of factors [23]. The secondary arc can be modeled by:

$$\frac{dg_s}{dt} = \frac{1}{T_s} (G_s - g_s) \quad (15)$$

where g_s is the time varying secondary arc conductance, T_s is the time constant of the secondary arc and G_s is the stationary secondary arc conductance.

The stationary secondary arc conductance is obtained by:

$$G_s = \frac{|i|}{V_s \ell_s(t_r)} \quad (16)$$

where V_s is the constant voltage parameter per unit length of secondary arc, $\ell_s(t_r)$ is the time varying length of secondary arc and $|i|$ is absolute value of the secondary arc current.

The time constant of the secondary arc can be defined as:

$$T_s = \frac{\beta I_s^{1.4}}{\ell_s(t_r)} \quad (17)$$

where the coefficient β is about 2.51×10^{-3} for low current arcs [23].

The secondary arc length variation is approximated by the following equation for relatively low wind velocities from 0-1 m/s:

$$\ell_s(t_r)/\ell_{s0} = \begin{cases} 10t_r & t_r > 0.1s \\ 1 & t_r \leq 0.1s \end{cases} \quad (18)$$

Furthermore, the re-ignition voltage (withstand voltage) has the complex characteristics of the secondary arc as described in [23]. The secondary arc can be

re-ignited if a sustaining arc energy voltage supplied by power system is larger than the re-ignition voltage. Based on the experimental results, the re-ignition voltage is obtained by Eq. 20 [23]:

$$V_r(t_r) = \left[5 + \frac{1620T_e}{2.15 + I_s} \right] \times (t_r - T_e) h(t_r - T_e) \times 10^3 \text{ V/cm} \quad (19)$$

where $V_r(t_r)$ is the arc re-ignition voltage that has to be reached before the arc restrikes again, T_e is time from the initiation of secondary arc to a current zero and $h(t_r - T_e)$ is a delayed unit-step function ($= 0$ when $t_r < T_e$, $= 1$ when $t_r > T_e$).

V. PROPOSED ALGORITHM

In the proposed algorithm, the faulted phase voltage signal is captured at a sampling rate of 20kHz. Then by using db8 wavelet packet, the voltage signal is decomposed to scale 8, and coefficients of node 257 (which contain frequency range between 78.125Hz to 117.1875Hz) and nodes 259 to 262 (which contain frequency range between 156.25Hz to 312.5Hz) are selected. Therefore the Index is obtained from:

$$Index = \sum_{\substack{k=257 \\ k \neq 258}}^{262} d_k(i)^2, \quad i = 1 : N \quad (20)$$

where, d_k and N are the coefficients and the number of coefficients at node k , respectively.

It should be noted that the Index is computed after the both line end breakers have isolated the faulted phase. Furthermore, this computation is delayed by one cycle to overcome the transient produced during opening period of the circuit breakers.

The behavior of proposed Index is completely different under arcing faults and permanent faults as shown in Figs. 4 and 5, respectively. It is supposed that an A-phase to earth fault occurs on the transmission line at an instant 0.3s and at 0.35s the faulty phase is isolated from both ends by opening the breakers. The fault location is 100km from the sending end of the line and load angle is 0° .

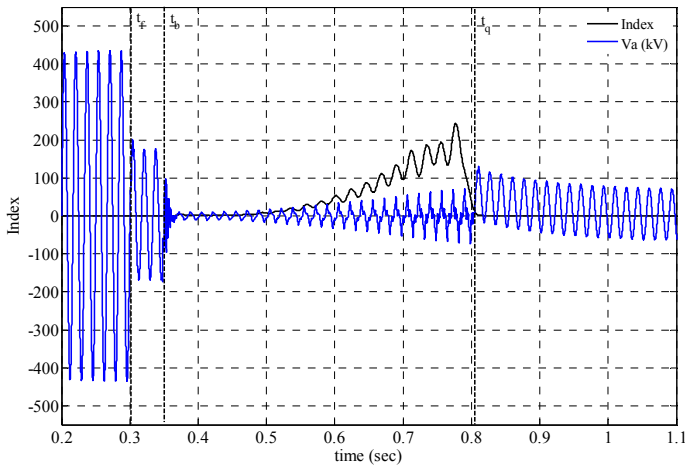


Fig. 4 Variation of Index during a single phase to earth transient fault. ($L_f=100\text{km}$, $t_f=0.3\text{s}$ and $\delta=00$)

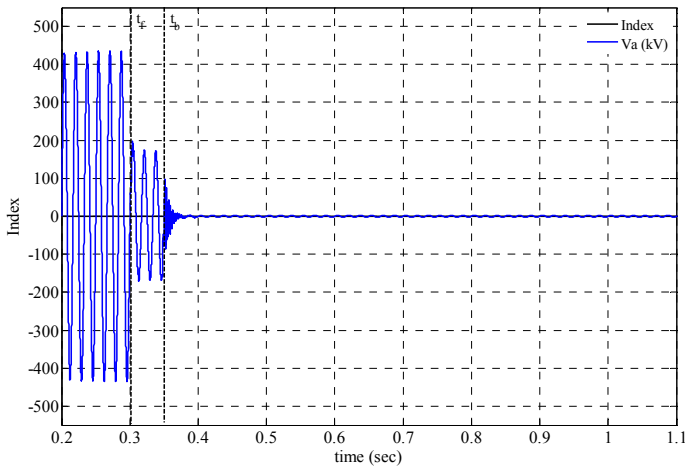


Fig. 5 Variation of Index during a single phase to earth permanent fault. ($L_f=100\text{km}$, $t_f=0.3\text{s}$ and $\delta=00$)

It can be seen in Fig. 4 that in case of transient faults after the breakers opening (instant t_b), Index has a non-zero value and whenever the secondary arc is quenched (instant t_q), its value becomes zero. However, it is obvious from Fig. 5 that during permanent faults Index remains equal to zero and does not change.

This feature has been used to distinguish between permanent and transient faults and to determine the instant of secondary arc extinction, i.e. after the breakers opening, if Index does not change and remains at the zero

value, it is a permanent fault, otherwise, the fault is recognized as a transient one and in this case as the secondary arc is quenched the value of the Index becomes zero.

Consequently, by evaluating the value of the proposed Index, the transient and permanent faults, as well as the secondary arc extinction time are identified.

In theory, to distinguish permanent faults from transient faults and to determine the secondary arc extinction time, the Index only needs to be compared with zero. In practice, Index is compared with a small value, α , to overcome low amplitude variations of the Index during permanent faults. In the 500kV simulated test system, the amount of α is considered 0.75.

VI. SIMULATION RESULTS

The proposed algorithm has been validated by numerous simulation tests under different fault conditions on the transmission line with/without reactor compensation. The fault conditions include different load angles, fault occurrence instants, and fault locations. Only some selected test results are given here for the purpose of brevity.

In the first case, it is assumed that a phase ‘a’ to earth fault occurs at the instant 0.302s and the distance of 200km from the sending end bus. The load angle is 0° and the breakers are opened at 0.352s. Fig. 6 shows the algorithm performance under this fault condition. Fig. 7 depicts the algorithm performance under permanent fault for the same condition.

As shown in Fig. 6, during arcing fault and after the breakers opening, Index has a non-zero value and as the secondary arc is quenched Index becomes zero. However, it is evident in Fig. 7 that during permanent faults, Index remains equal to zero and does not change.

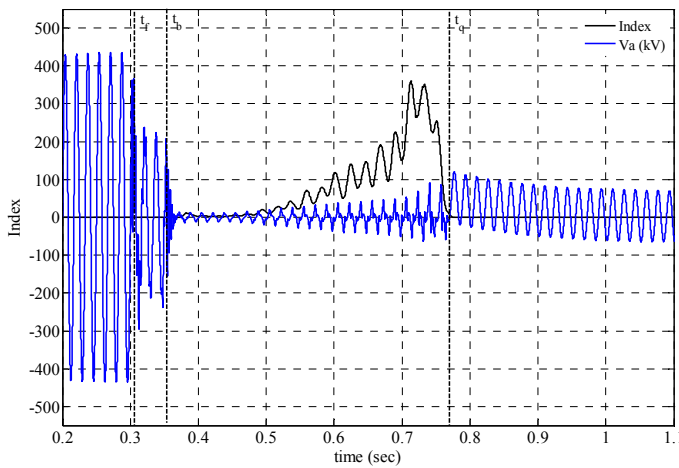


Fig. 6 Algorithm performance for a single phase to earth transient fault. ($L_f=200\text{km}$, $t_f=0.302\text{s}$ and $\delta=00$)

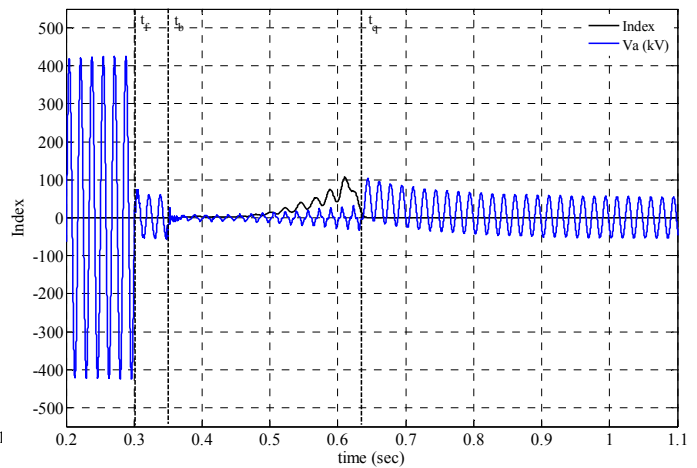


Fig. 8 Algorithm performance for a single phase to earth transient fault. ($L_f=20\text{km}$, $t_f=0.3\text{s}$ and $\delta=-200$)

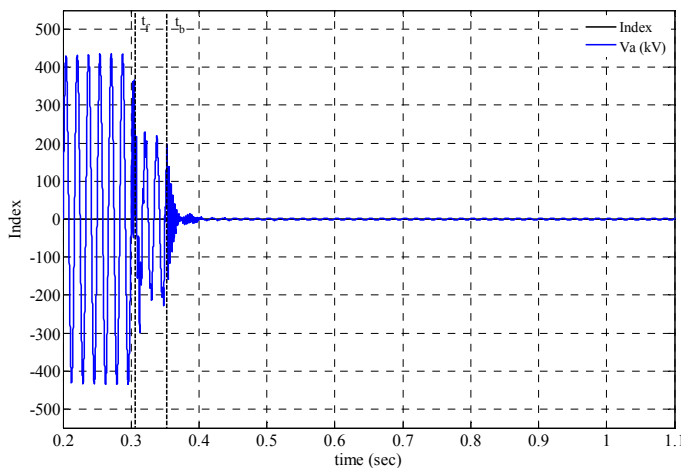


Fig. 7 Algorithm performance for a single phase to earth permanent fault ($L_f=200\text{km}$, $t_f=0.302\text{s}$ and $\delta=00$)

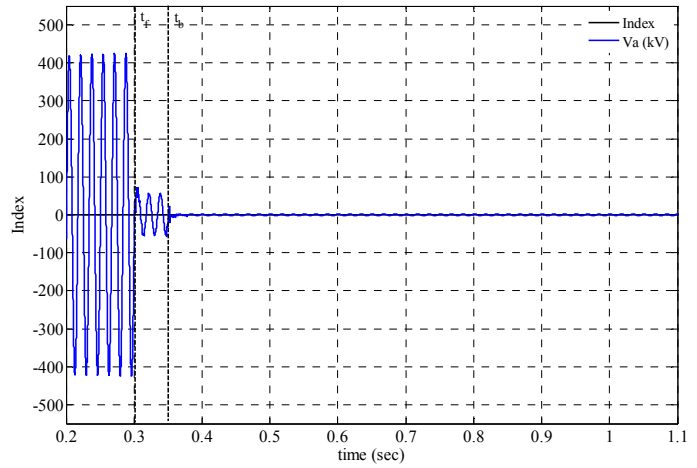


Fig. 9 Algorithm performance for a single phase to earth permanent fault. ($L_f=20\text{km}$, $t_f=0.3\text{s}$ and $\delta=-200$)

In the second case, it is assumed that the fault occurs at the instant 0.3s and the distance of 20km from the Bus 'A'. The both end breakers isolate the faulted phase at the instant 0.35s and the load angle is -20° . Fig. 8 shows the algorithm performance for the transient fault, whereas Fig. 9 illustrates the algorithm performance when the fault is permanent.

Figs. 4 to 9 show the validity of the algorithm for different load angles, fault locations and fault occurrence instants.

In the third case, it is supposed that 50MVAR shunt reactors with earthed neutrals are installed at both line ends and the fault occurs at the instant 0.306s and a distance of 120km from the Bus 'A'. The both end breakers isolate the faulted phase at the instant 0.356s and the load angle is 5° . Each 50MVAR reactor has been modeled by a resistance of $R=10\Omega$ in series with a reactance of $X=5000\Omega$.

Fig. 10 shows the algorithm performance under transient fault for this condition. Fig. 11

depicts the algorithm performance under permanent fault for the same condition.

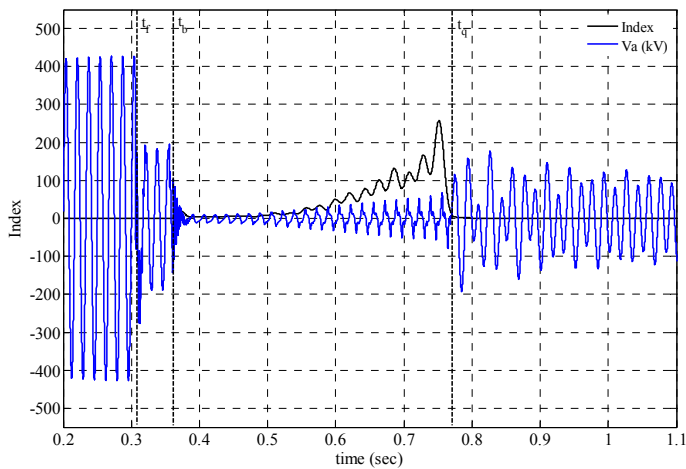


Fig. 10 Algorithm performance for transient fault on transmission line with earthed neutral shunt reactor. ($L_f=120\text{km}$, $t_f=0.306\text{s}$ and $\delta=50$)

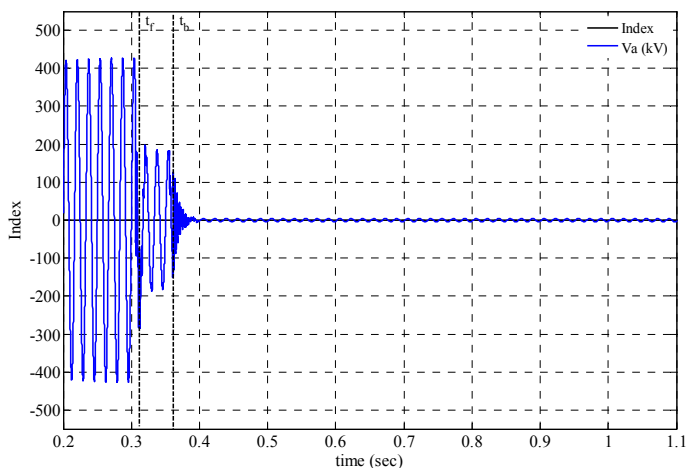


Fig. 11 Algorithm performance for permanent fault on transmission line with earthed neutral shunt reactor. ($L_f=120\text{km}$, $t_f=0.306\text{s}$ and $\delta=5^0$)

It can be seen that the algorithm can exactly determine the transient, permanent faults and the secondary arc extinction instant even for the shunt reactor compensated transmission line, which is a significant advantage of the proposed method.

VII. CONCLUSION

A new algorithm for adaptive single pole auto-reclosing has been proposed based on computing of an Index using WPT. The algorithm performs based on evaluating the value of the Index.

The proposed algorithm has the advantage that it can directly distinguish between transient and permanent faults and determine the instant of secondary arc extinction, and it does not require variant threshold level. Furthermore, the generated reclosing signal by the algorithm is independent of the fault location, line parameters and pre-fault operational conditions. Another advantage of the algorithm is that it can recognize the transient, permanent faults and the secondary arc extinction instant in shunt reactor compensated transmission lines.

The accuracy and sensitivity of the proposed algorithm have been verified by several simulation tests under different fault conditions.

VIII. REFERENCES

- [1] Power System Relaying Committee Working Group, "Single Phase Tripping and Auto Reclosing of Transmission Lines IEEE Committee Report," *IEEE Transactions on Power Delivery*, vol. 7, no. 1, pp. 182-192, January 1992.
- [2] S. P. Ahn, C. H. Kim, R. K. Aggarwal and A. T. Johns, "An alternative approach to adaptive single pole auto-reclosing in high voltage transmission systems based on variable dead time control," *IEEE Transactions on Power Delivery*, vol. 16, no. 4, pp. 676-686, October 2001.
- [3] Z. Q. Bo, R. K. Aggarwal and A. T. Johns, "A novel technique to distinguish between transient and permanent fault based on detection of current transients," Proceeding of 4th International Conference on Advances in Power System Control and Management, APSCOM-97, Hong Kong, pp. 217-220, November 1997.
- [4] C. E. J. Bowler, P. G. Brown and D. N. Walker, "Evaluation of the Effect of Power Circuit Breaker Reclosing Practices on Turbine-Generator Shafts," *IEEE Transactions on Power Apparatus and Systems*, vol. PAS-99, pp. 1764-1779, 1980.
- [5] G. Yaozhang, S. Fanghai, and X. Yuan, "Prediction methods for preventing single-phase reclosing on permanent fault," *IEEE Transactions on Power Delivery*, vol. 4, no. 1, pp. 114-121, January 1989.

- [6] X. Lin, H. Liu, H. Weng, W. Lu, P. Liu and Z. Q. Bo, "A Novel Adaptive Single-Phase Reclosure Scheme Using Dual-Window Transient Energy Ratio and Mathematical Morphology," *IEEE Transactions on Power Delivery*, vol. 21, no. 4, October 2006.
- [7] X. Lin, H. Liu, H. Weng, P. Liu, B. Wang, Z. Q. Bo, "A Dual-Window Transient Energy Ratio-Based Adaptive Single-Phase Reclosure Criterion for EHV Transmission Line," *IEEE Transactions on Power Delivery*, vol. 22, no. 4, pp. 2080-2086, October 2007.
- [8] R. K. Aggarwal, A. T. Johns, Y. H. Song, R. W. Dunn, D. S. Fitton, "Neural-Network Based Adaptive Single-Pole Autoreclosure Technique for EHV Transmission Systems," *IEE Proceedings on Generation Transmission and Distribution*, vol. 141, no. 2, pp. 155-160, March 1994.
- [9] D. S. Fitton, R. W. Dunn, R. K. Aggarwal, A. T. Johns, A. Bennett, "Design and implementation of an adaptive single pole autoreclosure technique for transmission lines using artificial neural networks," *IEEE Transactions on Power Delivery*, vol. 11, no. 2, pp. 748-755, April 1996.
- [10] I. K. Yu and Y. H. Song, "Wavelet Transform and neural network approach to developing adaptive single-pole auto-reclosing schemes for EHV transmission systems," *IEEE Power Engineering Review*, pp. 62-64, November 1998.
- [11] X. Lin and P. Liu, "Method of distinguishing between instant and permanent faults of transmission lines based on fuzzy decision," *IEEE International Conference on Energy Management and Power Delivery*, vol. 2, pp. 445-460, March 1998.
- [12] Z. M. Radojevic, J. R. Shin, "New digital algorithm for adaptive reclosing based on the calculation of the faulted phase voltage total harmonic distortion factor," *IEEE Transactions on Power Delivery*, vol. 22, no. 1, pp. 37-41, January 2007.
- [13] N. I. Elkalashy, H. A. Darwish, A. M. I. Taalab, M. A. Izzularab, "An adaptive single pole autoreclosure based on zero sequence power," *Electric Power Systems Research*, vol. 77, pp. 438-446, 2007.
- [14] امیر پرهام، صادق جمالی "الگوریتم عددی برای باز بست تطبیقی تک فاز با استفاده از ولتاژ توالی صفر"، بیست و دومین کنفرانس بین المللی برق، PSC2007، ایران، تهران، ۲۸-۳۰ آبان ۱۳۸۶.
- [15] S. A. Saleh, "A Wavelet Packet Transform-Based Differential Protection of Three-Phase Power Transformers," Master's Thesis, Memorial Univ. Newfoundland, St. John's, NF, Canada, 2003.
- [16] E. Y. Hamid and Z. I. Kawasaki, "Wavelet-based data compression for power disturbances using minimum description length data," *IEEE Transactions on Power Delivery*, vol. 17, no. 2, pp. 460-466, April 2002.
- [17] Matlab: Wavelet Tool Box, 1995. Mathworks, Ver. 6.1.
- [18] C. K. Chui, *Wavelets: A Mathematical Tool for Signal Processing*. Philadelphia, PA: SIAM, 1997.
- [19] A. M. Gaouda and M. M. A. Salama, "Power quality detection and classification using wavelet multi-resolution signal decomposition," *IEEE Transactions on Power Delivery*, vol. 14, no. 4, pp. 1469-1475, October 1999.
- [20] Y. Zhuang and J. S. Baras, "Optimal Wavelet Basis Selection for Signal Representation," *Center for Satellite and Hybrid Communication Networks*, CSHCN T.R. 94-7, 1994.
- [21] S. K. Pandey and L. Satish, "Multiresolution signal decomposition: A new tool for fault detection in power transformers during impulse tests," *IEEE Transactions on Power Delivery*, vol. 13, no. 4, pp. 1194-1200, November 1998.
- [22] L. Prikler, M. Kizilcay, G. Ban and P. Handl, "Improved Secondary Arc Models based on Identification of Arc Parameters from Staged Fault Test Records", in *Proc. 14th Power Systems Computation Conf.*, Session 24-Paper 3, June 2002.
- [23] A. T. Johns, R. K. Aggarwal and Y. Song, "Improved technique for modelling fault arcs on faulted EHV transmission systems," *IEE Proceedings on Generation Transmission and Distribution*, vol. 141, no. 2, pp. 148-154, March 1994.

[14] امیر پرهام، صادق جمالی "الگوریتم عددی برای باز بست تطبیقی تک فاز با استفاده از ولتاژ توالی صفر"، بیست و